# Distribution System Reconfiguration Analysis Under Different Load Demand Using ACO and PSO Algorithms

**Zahraa H. Dawood [a*], Prof. Dr. Rashid H. Al Rubayi [b*]**

[a] University of Technology, Iraq, **30553@student.uotechnology.edu.iq**

[b] University of Technology, Iraq, **30062@uotechnology.edu.iq**

Abstract— Optimal re-configuration is used to reduce power losses and keep the voltage within its allowable interval in power distribution systems considering voltage, current, and radial condition constraints. Effective optimization algorithms using 'Ant Colony Optimization (ACO) and Particle Swarm Optimization (PSO)' are presented and discussed to minimize power losses in distribution network by network re-configuration. The proposed model uses binary strings which represent the state of the network switches. The algorithms are applied and tested on 33-bus IEEE test systems to find the optimum configuration of the network with regard to power losses. Three different load scenarios are considered, and the effectiveness of the proposed techniques is also demonstrated with improvements in power loss reduction through MATLAB Under steady-state condition.

Text index— Re-configuration; ACO; PSO; radial structure; power loss minimization; voltage profile improvement.

## 1 INTRODUCTION

Distribution networks provide electricity for three types of essential loads: residential, commercial and manufacturing. The load profiles for each of these load types are different, which causes the distribution feeder to become more overloaded at some times of the day and less loaded at other times; and the operating conditions of the distribution network also change with this load variation. If not well compensated, the voltage at various buses goes out of recommended range and the actual loss on the feeders also rises, resulting in high system operating expenses. Moving the system loads may be used to reduce or eliminate system losses, alleviating overloading of network elements and to maintain the voltage in the power distribution network within their acceptable ranges by re-configuring the network from time to time in order to re-distribute the load currents more effectively [1].

Placement of capacitors, grading of conductors, re-configuration of feeders and allocation of distributed generators (DG) are effective strategies to reduce the Power loss [2]. Adding these strategies to the distribution network needs a large price of installation. Re-configuration of the system could be implemented through re-configuring sectionalizing switches and tie switches. This process reduces power loss and also enhances the profile of voltage by taking into account operating bonds with no extra cost [3].

As the distribution network consists of several switches and the amount of switching operations available is immense. Network re-configuration is thus a very difficult problem in decision-making. At the other hand, the constraint of radially and the discrete nature of the switch values prohibit the use of classic optimization techniques to solve the re-configuration problem. Therefore, most algorithms are based on heuristic search techniques, using either analytical or knowledge-based engines [4]. which they attempt to find a near – optimum solution for large power systems within reasonable time.

Over the last two decades, several researchers have solved the issue of network re-configuration using various approaches with the goal of minimizing power loss and/or improving the voltage profile of power distribution networks, as shown in Fig.1 [5].

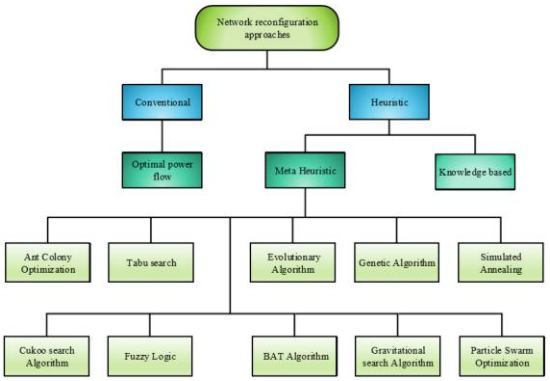


Fig. 1: Classification of network reconfiguration approaches

The distribution system re-configuration for reducing network losses was first suggested by Merlin and Back in 1975 [6]. Subsequently, significant research has been carried out in this field to make network re-configuration more efficient. Numerous methods such as PSO, Tabu Search (TS), knowledge-based expert system, simulated annealing (SA),

single-loop optimization, Ant Colony Optimization (ACO) and Harmony Search Algorithm (HS) have been suggested in the literature [7-12].

The minimization of the actual loss of power is used as an objective function. The proposed approaches are tested on standard 33-bus test systems and the simulation results indicate the good performance of the proposed techniques.

The material of this paper is arranged as follows: The problem formulation of the distribution system re-configuration is described in Section 2. Section 3 explains the algorithms that was suggested here. The test system is explained in section 4. The results of the simulation are summarized and discussed in Section 5. This paper ends with some observations and conclusions.

## 2 Network Re-configuration Problem Formulation

Network re-configuration refers to physical or electrical modification of current network. Examples of network re-configuration include changing routes of transmission and distribution lines, bifurcation of distribution feeders, shifting of load to other less loaded feeders and adjusting system operating voltages. When operational conditions change, network re-configuration is achieved by opening / closing the network switches under a number of restrictions that should not be violated after re-configuration. The constraints are:

- Operating in radial form
- All loads are served.
- Lines, transformers, and other equipment's operate within their current capacity limits.
- Bus voltage within regulatory limits.

### 2.1 Load Flow Calculations Using Backward / Forward Sweep

The network load flow from two sets of recursive equations can be determined iteratively. The first set of equations for the calculation of the power flow through the branches, starting from the last branch and continuing backward towards the root node. The other set of equations is to measure the voltage magnitude and angle of each node starting from the root node and moving forward in the direction of the last node. The fig. 2 shows the representation of two nodes in a distribution line. Consider a branch 'j' is connected between the nodes 'i' and 'i+1'.

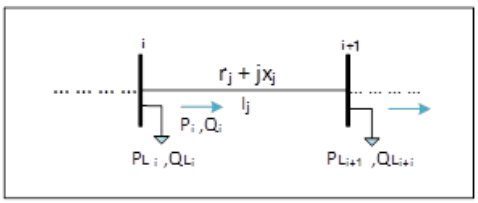


Fig. 2: Representation of two nodes in a distribution line

The effective active ( $P_i$ ) and reactive ($Q_i$) powers that of flowing through branch 'j' from node 'i' to node 'i+1' can be calculated backwards from the last node and is given as,

$$P_i = P'_{i+1} + r_j \frac{(P'^2_{i+1} + Q'^2_{i+1})}{V^2_{i+1}} \quad \ldots (1)$$

$$Q_i = Q'_{i+1} + x_j \frac{(P'^2_{i+1} + Q'^2_{i+1})}{V^2_{i+1}} \quad \ldots (2)$$

Where:

$P'_{i+1} = P_{i+1} + P_{Li+1}$ and $Q'_{i+1} = Q_{i+1} + Q_{Li+1}$
$P_{Li+1}$ and $Q_{Li+1}$ are loads that are connected at node 'i+1'.
$P_{i+1}$ and $Q_{i+1}$ are the effective real and reactive power flows from node 'i+1'.

The voltage magnitude and angle at each node are calculated in forward direction. Consider a voltage $V_i \angle \delta_i$ at node 'i' and $V_{i+1} \angle \delta_{i+1}$ at node 'i+1', then the current flowing through the branch 'j' having an impedance, $z_j = r_j + jx_j$ connected between 'i' and 'i+1'is given as,

$$I_j = \frac{V_i \angle \delta_i - V_{i+1} \angle \delta_{i+1}}{r_j + jx_j} \quad \ldots (3)$$

The total real and reactive power loss of radial distribution system can be calculated as,

$$TPL = \sum_{j=1}^{N_b} r_j \frac{(P_i^2 + Q_i^2)}{V_i^2} \quad \ldots (4)$$

$$TQL = \sum_{j=1}^{N_b} x_j \frac{(P_i^2 + Q_i^2)}{V_i^2} \quad \ldots (5)$$

At first, a flat voltage profile is assumed at all nodes i.e., 1.0 $pu$. The branch powers are calculated iteratively with the updated voltages at each node.

### 2.2 Objective Function

An aim of re-configuring the distribution network throughout usual operation would be to choose the ideal switch process policy to minimize loss of power and to keep the voltage in power distribution systems within its permissible interval. Also, Subsequent goals can be fulfilled by network re-configuration such as:

- Balancing feeder loads and helping to handle network overload situations by transferring loads from highly loaded feeders to lightly loaded feeders.
- Restoration of service under faulty conditions, thus enhancing system protection, reliability and improving power efficiency.
- Restoration of Service for maintenance.

In this paper, the problem of optimization is done on the basis of the reduction of power loss and the improvement of the voltage profile, taking into account restrictions and

different scenarios of load fluctuations. The objective function applied to find the minimum value of total power loss is shown in Equation (5): [13]

$$F(x) = min(TPL) \quad \ldots(5)$$

$$x = [Tie_1; Tie_2; \ldots\ldots; Tie_{Ntie}; Sw_1; Sw_2; \ldots\ldots Sw_{Ntie}]$$

where $x$ is the control variables vector; $Tie_i$is the state of the $ith$ tie switch; and $Sw_i$ is the switch.

Many similar distribution network re-configuration algorithms combine the TPL index with the minimum voltage index as an optimal multi-objective issue. The proposed objective is a mono-objective function; therefore, the design is more rational. According to the following case study, it is revealed that the algorithm being compared with the proposed algorithm cannot achieve the minimum TPL because of the index voltage compromise. In fact, looking for a voltage that is as high as possible in range is irrational. The explanation lies in the fact that the utility has provided the consumer with the appropriate power by means of the permissible voltage range limitation. Accordingly, the company needs to achieve the full benefit, i.e. the single minimum TPL should be a reasonable target. As regards the power quality, which is different from the minimum voltage, it should be replaced by the average voltage index, which should be a reasonable index for the determination of the power quality from the point of view of the utility and the users [13].

## 2.3 Average Voltage Concept

The $V_{min}$index is commonly used for voltage analysis in the distribution network. In the network re-configuration analysis, the $V_{min}$index is not good enough to select the best solution, as the negative power compensation resources are insufficient to raise the $V_{min}$ above 0.95, which is the minimum voltage allowed. Furthermore, it is difficult to deal with certain bus voltages in order to determine whether or not there has been an increase in the voltage in the distribution network, as voltage improvements may have occurred in some busses and not in others, or may have deteriorated in some busses. A new average voltage index is offered in this study to manage all bus voltages and to fulfill most of the electrical power constraints. The index is given in Equation (6):

$$V_{av} = \frac{\sum_{i=1}^{N_n} V_i}{N_n} \quad \ldots(6)$$

where $V_{av}$ is the average voltage of the system; $V_i$ is the voltage magnitude of the $ith$ bus; $Nn$ is the number of network buses.[13]

## 2.4 Constraint

In order to measure system power losses, bus voltages, and branch current, the power flow analysis shall be performed for each proposed configuration. The goal function is limited to the following:

1. Bus Voltage will be between the upper and lower limits as shown in equation (7).

$$v_{i,min} \le |v_i| \le v_{i,max} \quad i = 1,2,\ldots,N_n \quad \ldots(7)$$

Where: $v_i$ is the voltage magnitude of the $ith$ bus, $v_i^{max}$and $v_i^{min}$ are the minimum and maximum voltage magnitude boundaries of the $ith$ bus.

2. Power flow at each branch must be below or equal to its maximum capacity, as shown in equation (8)

$$S_j \le S_j^{max} \quad \ldots(8)$$

3. Branch current limit:

$$|I_j| \le I_{max} \quad \ldots(9)$$

Where: $|I_j|$ is the current magnitude flowing in the branch $j$, $I_{max}$ is the maximum permissible current limit.

4. Since most distribution systems operate in a radial topology as a compromise between operating costs (mainly related to protection systems) and the reliability, radial topology is seen as a restriction.

## 2.5 Load Demand Variation

The loading of the network is a customer-type function, as such differing daily and seasonal load curves, Load profiles fluctuates from feeder to feeder due to the mixing and dispersion of the customer service [14]. Sectionalizing switches installed to separate the line section of each distribution line and the tie switches installed at the distribution line connection points. By re-locating existing switches, the distribution system can be changed to a new network topology with minimal power losses and an improved voltage profile compared to the previous one [1]. Choosing and positioning a sufficient number of switches is a daunting activity in the planning of distributions. In addition, the switches installed in the distribution networks are operated flexibly, according to the expansion of the load and the network. In this article, the superiority and efficiency of the proposed approach is evaluated in three separate cases:

- Case 1: constant load
- Case 2: Various Load Rates
- Case 3: Different Load Patterns

### 2.5.1 Different Load Levels

The load requirements (active and reactive) in the buses are linearly shifted from low loads ($\gamma$ =0.75) to the

highest load demand point ($\gamma$ =1.25) with a step change of 12.5%. For each load demand level, the status of the switches opened, total active and reactive power losses, total apparent power losses, minimum voltage and average voltages are determined in various configurations. Where the solution suggested enables distribution system engineers to choose the optimal configuration that result in a substantially decreased in power loss response to fluctuations in the load demand level by $\gamma$. Load demand fluctuates as in equations (10) and (11).[13]

$$PL_i = \gamma\, PL_{io} \quad \ldots (10)$$

$$QL_i = \gamma\, QL_{io} \quad \ldots (11)$$

where $\gamma$ is the value of the load variance ratio; and $PL_{io}$ and $QL_{io}$ are the reference constant active and reactive power of the $ith$ load.

### 2.5.2 Different Load Patterns

Present electrical utilities form a complex blend of static and dynamic components that work in a variety of configurations [15]. A constant load model can be defined as a polynomial load representing voltage magnitude and frequency power ratio [16]. As shown in Equations (12) and (13), the common form of a load model consisting of actual and reactive power dependence on voltage ($V$) and frequency ($f$):

$$PL_i = f_{PL}(V, f) \quad \ldots (12)$$

$$QL_i = f_{QL}(V, f) \quad \ldots (13)$$

Where ($PL_i$) and ($QL_i$) are the active and reactive load demand; $f_{PL}$, $f_{QL}$ are the functions of active and reactive load demand of the system.

Frequency load dependence is often overlooked, as voltage variations are often more common and observable than system frequency variations [17]. The main network connection in this work maintains the frequency constant; thus equations (14) and (15) represent the load model based on the variations in the bus voltages. Load demands have been updated to depend on voltage, and system re-configuration has been adjusted to the network bus voltage profile. As a result, demand action has changed with the re-configuration of the network. In order to execute the actual active and reactive load, the load was defined as voltage-dependent as indicated in Equations (14) and (15).

$$PL_i = PL_{i0}\left[p_1\left(\frac{V_i}{V_{i0}}\right)^2 + p_2 + p_3\left(\frac{V_i}{V_{i0}}\right)^0\right] \quad \ldots (14)$$

$$QL_i = QL_{i0}\left[q_1\left(\frac{V_i}{V_{i0}}\right)^2 + q_2 + q_3\left(\frac{V_i}{V_{i0}}\right)^0\right] \quad \ldots (15)$$

$$p_1 + p_2 + p_3 = 1 \quad \ldots (16)$$

$$q_1 + q_2 + q_3 = 1 \quad \ldots (17)$$

In addition, equations (14) and (15) characterize the ZIP model, where Z, I and P denote the load elements of constant impedance, constant current and constant power, respectively. The parameters ($p_1$ and $q_1$), ($p_2$ and $q_2$), and ($p_3$ and $q_3$) in Equations (16) and (17) indicate the relative involvement of constant impedance load, constant current load, and constant power for active and reactive loads, respectively. $PL_{i0}$ and $QL_{i0}$ are the references of active and reactive power of the $ith$ consumer at rated voltage $V_{i0}$ = 1 per unit. $V_i$ is the per unit delivering voltage of the $ith$ consumer.

Equations (14) and (15) can be modified as Equations (18) and (19), respectively, for the voltage-exponential load.

$$PL_i = PL_{i0}\left[\left(\frac{V_0}{V_{i0}}\right)^{\sigma}\right] \quad \ldots (18)$$

$$QL_i = QL_{i0}\left[\left(\frac{V_i}{V_{i0}}\right)^{\tau}\right] \quad \ldots (19)$$

Where

$$\sigma \cong \frac{p_1 \times 2 + p_2 \times 1 + p_3 \times 0}{p_1 + p_2 + p_3} \quad \ldots (20)$$

$$\tau \cong \frac{q_1 \times 2 + q_2 \times 1 + q_3 \times 0}{q_1 + q_2 + q_3} \quad \ldots (21)$$

Equations (18) and (19) σ and τ denote the voltage-exposing features of the active ($PL_i$) and reactive ($QL_i$) load requirements, respectively; σ and τ can be computed from equations (20) and (21) respectively. The values of the active and reactive power exponents used for this work are shown in Table 1.

TABLE 1
Type of loads and the exponent values [18]

| Load Type | condition | σ | τ |
|---|---|---|---|
| Residential Consumer | Spring and Summer/Day | 0.72 | 2.96 |
| | Spring and Summer/Night | 0.92 | 4.04 |
| | Autumn and Winter/Day | 1.04 | 4.19 |
| | Autumn and Winter/Night | 1.30 | 4.38 |
| Commercial Consumer | Spring and Summer/Day | 1.25 | 3.50 |
| | Spring and Summer/Night | 0.99 | 3.95 |
| | Autumn and Winter/Day | 1.50 | 3.15 |
| | Autumn and Winter/Night | 1.51 | 3.40 |

## 3 The Proposed Methods:

### 3.1 Ant Colony Optimization (ACO) Method

The first ant colony optimization (ACO) algorithm used by Dorigo [19] in 1992. In recent years, some modifications have made this met heuristic an effective tool for solving combinatorial optimization problems. Some of the recently proposed ACO applications in the distribution system region concern feeder restoration and optimum switching adaptations for distribution system planning. [1]

The inspiring source of ACO is the pheromone trail laying and following behavior of real ants which use pheromone as a communication medium. the algorithm can find the optimum solution by generating artificial ants. As the real ants search their environment for food, the artificial ants search the solution space [20]. artificial ants, mediated by artificial pheromone trails, the pheromone trails in ACO serve as distributed, numerical information [21], any pheromone-rich path will thus become the path of the target. The procedure is illustrated by Fig. 3 [22], In Fig. 3 (a), The ants move straightaway from food source A to nest B. When an obstacle comes up as shown in Fig. 3(b), the path is cut off. In their movements, the ants will not be able to follow the previous trail. In this situation, they have the same probability to go right or left. But after some time, the path CD will have more pheromones and all the ants will move in the path ACD.

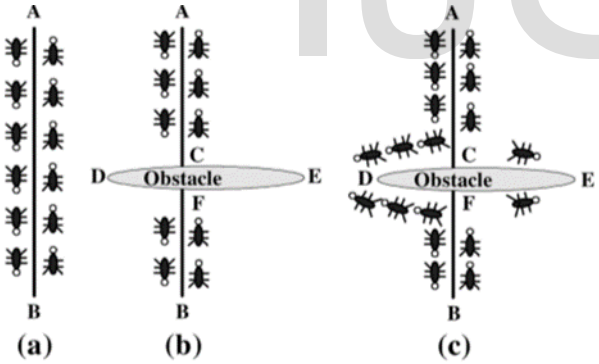


Fig. 3: The behavior of real ants

As the ants from C to reach F through D will reach more rapidly than that of the ants through E, i.e., CEF. Hence ant at F from B will find pheromone a path FDCA and will go through it, where Fig. 3 (c) illustrates that the shorter path CDF will collect more amount of pheromone than the longer path CEF. As a result, more and more ants will be directed to move along the shorter path. Due to this auto-catalytic process, all ants will soon choose a shorter path. This behavior is the basic concept of an ant colony algorithm. The proposed ACO algorithm that is presented here is shown in the flow chart of fig. 4, the following steps give details to the flow chart:

1. To create meshed loops, close all the tie and sectionalizing switches in the network. The number of meshed loops is equal to the number of tie switches.
2. Generate arbitrary number of artificial ants.
3. Initialize the parameters, heuristic parameter (ß), pheromone parameter ($\alpha$), evaporation parameter (ϱ) for local updating rule, evaporation factor (μ) for global updating rule, and initial pheromone values for each switch.
4. State transition rule:

Ants choice their next state (switch) according to this rule given by (22)

$$S_K(i,j) = \begin{Bmatrix} s_1 \; if \; q \le q_o \\ s_2 otherwise \end{Bmatrix} \quad \dots (22)$$

$$S_1 = argmax \; [\; [t(i,j)]^a \cdot \; [h(i,j)]^b] \quad \dots (23)$$

Where:

$S_k(i,j)$ is the state (switch) that $ant_k$ chooses in its next move; $k$ is the ant; $i$ and $j$ are the current and next state respectively; $S_1$ and $S_2$ are random variables represent the state (switch) that $ant_k$ selects according to transition state transition rule; $t(i,j)$ is the pheromone deposited by ants during move; $q$ is a random number uniformly distributed in [0,1];$q_0$ is a parameter between 0 and 1($0 \le q_0 \le 1$) according to equation (25); $h(i,j)$ is the heuristic information of the problem; $\alpha$ is a parameter represents the importance of pheromone; $\beta$ is a parameter represents the importance of heuristic; $S_2$ is selected according to a pseudo random rule or a pseudo random proportional rule given by (24).

$$S_2 = \frac{[\; [t(i,j)]^a \cdot \; [h(i,j)]^b]}{\sum_{l \in N_k(i)} [\; [t(i,l)]^a \cdot \; [h(i,l)]^b]} \; if \; j \in N_k(i) \quad \dots (24)$$

$$q_0 = \begin{vmatrix} c_1 \; if & 0 \le cycle \le n_0 \\ c_0 \; if & n_0 \le cycle \le n_1 \\ c_2 \; if & n_2 \le cycle \le n_{max} \end{vmatrix} \quad \dots (25)$$

Where:

$N_k(i)$ is the set of states (switches) that selected by ant k that is called tabu list; $n_0$ and $n_1$ are iteration frequency; $n_{max}$ is maximum iteration frequency; $c_0$ is a parameter its value between 0 and 0.4; $c_1$ is a parameter its value between 0.8 and 1.

5. Calculation of the Objective function:

The objective function is determined after the ants have finished selecting the switches (states) as given in equations in (5).

6. Local updating pheromone rule:

While constructing a solution each ant adjusts the pheromone by this rule given by (26).

$$t(i,j) = (1-\Gamma)\cdot\ t(i,j) + \Gamma \cdot t_0 \qquad \ldots(26)$$

Where:

$t_0$ is the initial value of pheromone; $\Gamma$ is a heuristically defined parameter; The local updating rule shuffles the search process.

7. Global updating pheromone rule:

Once all the ants have completed their tour (an iteration), this rule applies to the states (switches) belonging to the best solution. This rule offers the best solution for a large amount of pheromone and is given by (27):

$$t(i,j) = (1-\mathcal{M})\cdot t(i,j) + \mathcal{M}\sum_{k=1}^{m}\Delta t\ (i,j) \qquad \ldots(27)$$

$$\Delta t\ (i,j) = \begin{vmatrix} \frac{Q}{L_K} & if\ ant_k\ selects\ the\ edge\ or\ state\ (i,j) \\ 0 & otherwise \end{vmatrix} \ldots(28)$$

Where

$\Delta t\ (i,j)$ is the change in the pheromone; $\mathcal{M}$ is the pheromone evaporation factor; $Q$ is a constant between 1 and 10,000; $L_K$ is the best objective function solved by $ant_k$; $m$ is the number of states.

8. Repeat step 4 to step 6 continuously until satisfying the condition of abort iteration.
9. Up to abort iteration, the solution of minimum objective function in all local optimum solution is global optimum solution.

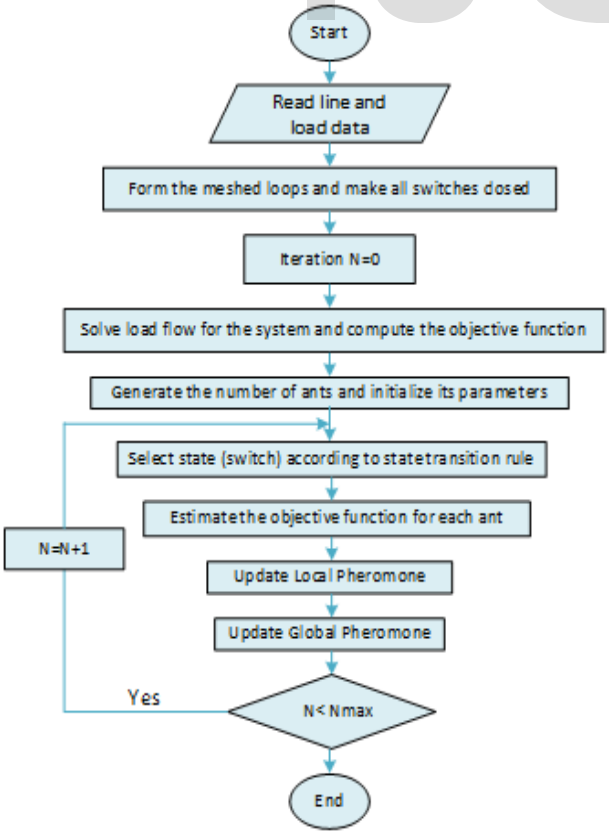


Fig. 4: Flow chart of the proposed algorithm

## 3.2 Particle Swarm Optimization (PSO) Method

In the year 1995, a new evolutionary computation technique called Particle Swarm Optimization (PSO) was proposed by Kennedy (social-psychologist) and Eberhart (electrical engineer) [23].

The main idea of the PSO is based on the social behavior (foraging) of organisms such as fish (schooling) and bird (flocking) [24,25]. The birds or fish will move to the food in certain speed or position. Their movement will depend on their own experience and experience from other 'friends' in the group ($pbest$ and $gbest$).

PSO implements the particle population first at random, where each particle represents a potential solution to the objective function under consideration. Each particle in the swarm can memorize its current position that is determined by evaluation of the objective function, velocity, and the best position visited during its flying tour in the problem search space referred to as "personal best position" ($pbest$). Here it is meant by the personal best position, the one that yields the highest fitness value for that particle. For a minimization task, the position having a smaller function value is regarded to as having a higher fitness [26]. Also, the best position visited by all particles is memorized, *i.e.* the best position among all $pbest$ positions referred to as "global best position" ($gbest$). One of the most widely used improvements is the introduction of inertia weight by Shi and Eberhart, which is employed to control the impact of the previous history of velocities on the current one [27]. The inertia weight location in the formulation will modify the search regions. A higher inertia weight will drive algorithm towards the global search, and a lower one will cause the PSO to search locally.

The Position and velocity of each particle are updated as follows:

$$v_i^{k+1} = w\ v_i^k + c_1 \times rand() \times \left(\frac{Pbest_i - x_i^k}{\Delta t}\right) + c_2 \times rand() \times \left(\frac{gbest_i - x_i^k}{\Delta t}\right) \ldots(29)$$

$$x_i^{k+1} = x_i^k + v_i^{k+1} * \Delta t \qquad \ldots(30)$$

Where:

$v_i^{k+1}$ : is the new velocity of $ith$ particle; $v_i^k$ : is the original velocity of $ith$ particle; $w$: is the inertia weight and is usually set to 1 or is changing with time; $rand()$: is a random number between 0 and 1; $x_i^k$: is the current position in the $ith$ dimension; $c_1, c_2$: are the acceleration coefficients; $pbest_i$: is the personal best position in the $ith$ dimension; $gbest_i$: is the global best position in the $ith$ dimension; $\Delta t$:is the time step.

It is a common practice in PSO literature to choose a unity time step ($\Delta t$), The personal best position is updated after $k$ iterations according to:

$$pbest^{k+1} = \begin{cases} pbest^{k} & if\ F\ (x^{k+1}) \geq F\ (pbest^{k}) \\ x^{k+1} & if\ F(x^{k+1}) < F\ (pbest^{k}) \end{cases} \quad \ldots (31)$$

Where:

$F$ : is the fitness function

Referring to (29), the velocity update equation has three terms; the first term represents the particle's memory of its current velocity (change in position) in the different dimensions of the search space, the second term is associated with "*cognition*" since it only takes into account the particle's own experience, while the third one represents the "*social interaction*" between the particles. Each agent updates each location according to the interaction of the above three components.

The particles are allowed to search the solution space until the maximum number of iterations is reached or a convergence criterion is satisfied. The global best at the end of the evolution is taken as the solution to the problem [28].

The proposed PSO algorithm that is introduced here is shown in the flow chart of figure 5. The following steps give explanations to the flow chart.

1. Input data of a distribution system including all the operational constraints and initialize a population of particles with random positions and velocities on dimensions in the space.
2. For each particle, evaluate the desired optimization fitness function (power loss) if it is better than the $pbest$, the value is set to $pbest$. If the best fitness better than the $gbest$, the value is set to $gbest$.
3. Store the particle with the best fitness ($gbest$) value by running the load flow program after checking radiality.
4. Change the velocity and position of the particle according to equations (29) and (30).
5. If $gbest$ is optimal solution then stop. Else go to Step 2.
6. End.

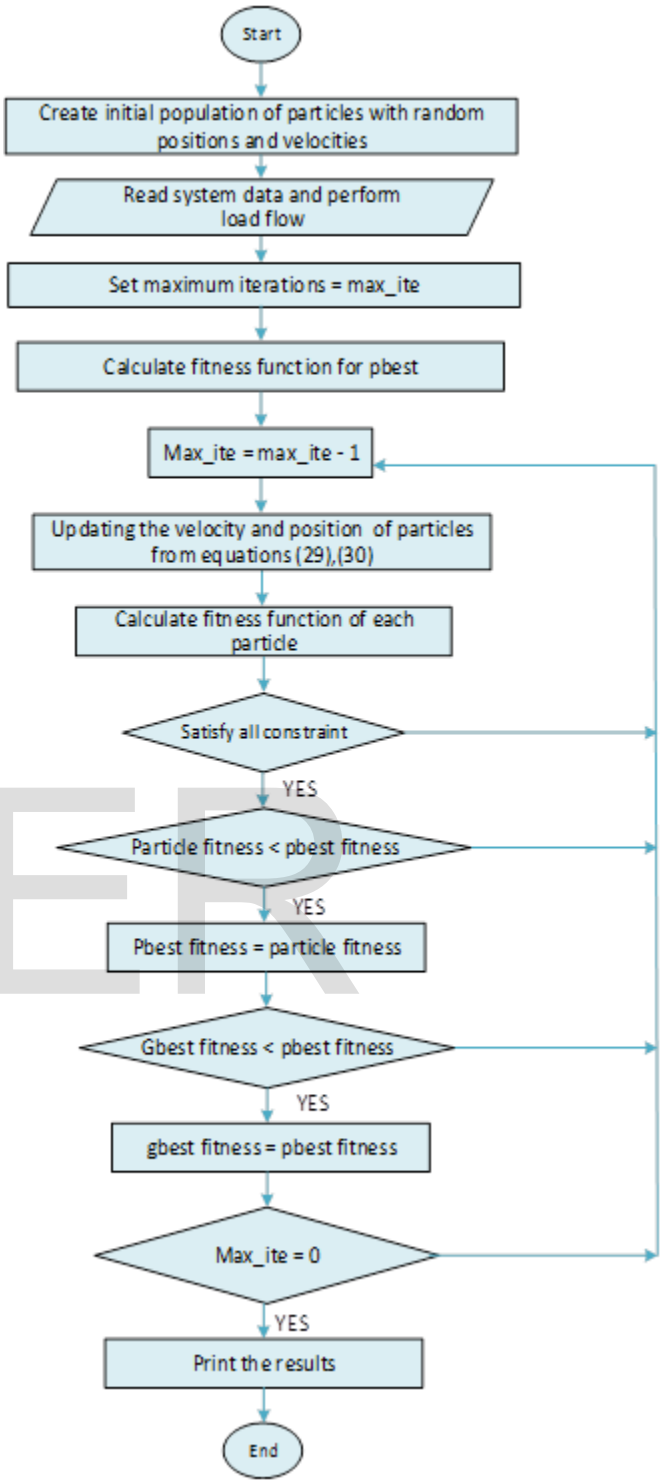


Fig. 5: Flow Chart of the Particle Swarm Optimization (PSO) Algorithm

## 4 Test System

The base configuration of the IEEE 33-bus distribution system used in simulation is depicted in Figure 6. The line and load data of this system are provided in reference [29]. It consists of one feeder, 33 buses, 5 normally open switches

are Sw33 to Sw37 (tie switches), represented by dashed lines and 32 normally closed switches (sectionalizing switches), Sw1 to Sw32, are represented by solid lines. The nominal system voltage is 12.66 kV, *Sbase* is 100 MVA and the total system loads are 3715 kW and 2300kVAr [30].

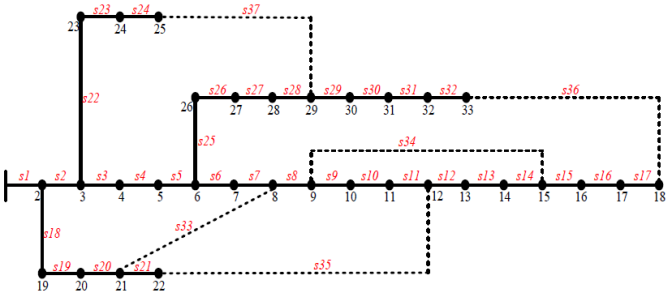

**Fig. 6:** The 33- bus network before re-configuration

For the three different load scenarios of the standard test system, when ACO approach is applied, a group of 100 ants are generated to construct the feasible solution of the system in each iteration; where the maximum number of iterations is 60 and when PSO approach is applied, a group of 100 particles are generated to construct the feasible solution of the system in each iteration; where the maximum number of iterations is 60. The parameters of ACO and PSO methods which they selected by the trial and error approach are illustrated in tables 2 and 3 below:

TABLE 2
The parameters of ACO

| ACO Method Parameters | | | | |
|---|---|---|---|---|
| | α | ß | ρ | μ |
| Case 1 | 0.8 | 0.2 | 0.7 | 0.8 |
| Case 2 | 0.8 | 0.2 | 0.7 | 0.8 |
| Case 3 | 1.1 | 0.009 | 1 | 15.5 |

TABLE 3
1 The parameters of PSO

| PSO Method Parameters | | | |
|---|---|---|---|
| | $w$ | $c_1$ | $c_2$ |
| Case 1 | 0.9 | 1.2 | 0.12 |
| Case 2 | 0.9 | 1.2 | 0.12 |
| Case 3 | 0.9 | 0.9 | 0.12 |

## 5 Simulation Results and Discussion

### 5.1 Optimal Re-configuration Results for case 1

Network re-configuration based on constant load demand for the standard IEEE 33-bus test network is implemented by using the proposed ACO and PSO algorithms. The results are summarized in Table 4.

Table 4
Results of the 33-bus network at constant load demands ($\sigma = 0, \tau = 0$), $\gamma = 1$

| Approaches | Open state | $TPL$ $(kW)$ | $TQL$ $(kVar)$ | $TSL$ $(kVA)$ | $V_{av}$ $(p.u.)$ | $V_{min}$ $(p.u.)$ |
|---|---|---|---|---|---|---|
| Initial configuration | Sw33, Sw34, Sw35, Sw36, Sw37 | 202.67 | 135.14 | 243.60 | 0.9485 | 0.9092 |
| (PSO) | Sw07, Sw09, Sw14, Sw28, Sw32 | 139.9799 | 104.9763 | 176.3632 | 0.9674 | 0.9413 |
| (ACO) | Sw07, Sw09, Sw14, Sw32, Sw37 | 139.5529 | 102.3962 | 174.7828 | 0.9652 | 0.9378 |

Table 4 explains the contrast between the proposed algorithms (ACO) and particle swarm optimization (PSO) algorithm, regarding the switch's status, active power loss, reactive power loss, apparent power loss, average voltage and minimum voltage. It was noticed that the best re-configuration of switches set was (Sw7, Sw9, Sw14, Sw32, Sw37) for standard 33-bus test network with constant feeder load demands because of its minimum TPL. It was also observed that both the TQL and TSL for the optimal set were the minima, while $V_{av}$ meets the code voltage restriction. The active power loss of the ideal re-configuration compared with the original case, showed a reduction of active power loss by 31.14279 % from 202.6700 $kW$ to 139.5529 $kW$ with a net decrease of active power loss being 63.1171 $kW$. The minimum voltage was improved by 2.86 % from 0.9092 $p.u.$ to 0.9378 $p.u.$

The voltage and active power loss reduction profiles of the network at constant load demand (for the initial and optimal configuration), when ACO algorithm is applied are shown in Fig. 7 and fig. 8. It can be seen that the voltage profile at all buses (except for buses 19, 20, 21, 22) were enhanced after reconfiguration.

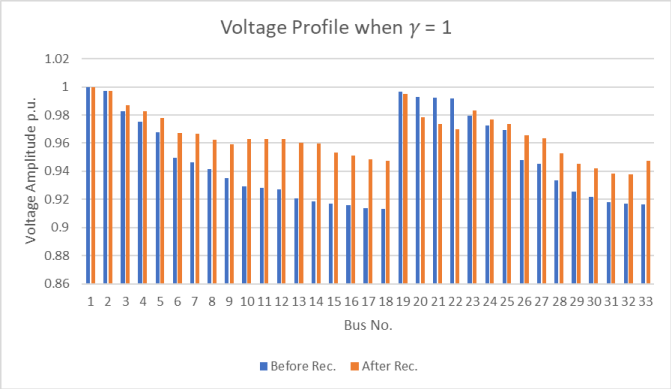


Fig. 7: Voltage profile for standard 33-bus system (before and after re-configuration) using the ACO algorithm at constant load demands when $(\sigma = 0, \tau = 0)$, $\gamma = 1$.

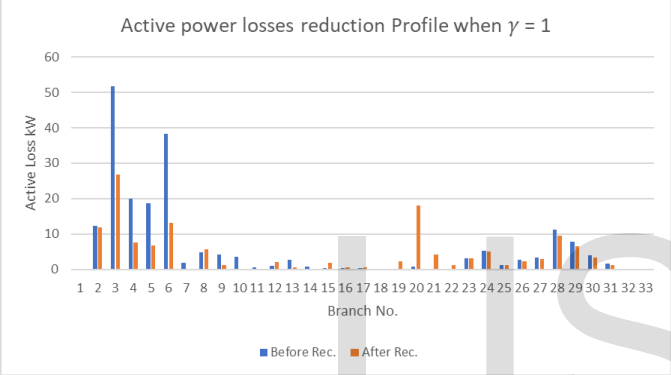


Fig. 8: Active power losses reduction profile for the 33-bus network (before and after re-configuration) using the ACO algorithm at constant load demands when $(\sigma = 0, \tau = 0)$, $\gamma = 1$

## 5.2 Optimal Re-configuration Results for Case 2

There are four levels of load demand starting from $\gamma = 0.75$ to $\gamma = 1.25$ with step changes of 12.5%. Tables 5-8 show that for standard 33-bus test network at each load level, the switch set (Sw7, Sw9, Sw14, Sw32, Sw37) had the minimum TPL. It was also observed that both the TQL and TSL for the optimal set were the minima for Tables 5-8.

TABLE 5
The 33-bus network results with load factor $\gamma = 0.75$.

| Approaches | Open state | $TPL$ $(kW)$ | $TQL$ $(kVar)$ | $TSL$ $(kVA)$ | $V_{av}$ $(p.u.)$ | $V_{min}$ $(p.u.)$ |
|---|---|---|---|---|---|---|
| Initial configuration | Sw33, Sw34, Sw35, Sw36, Sw37 | 109.7538 | 73.13 | 131.89 | 0.9621 | 0.9231 |
| (PSO) | Sw07, Sw11, Sw14, Sw32, Sw37 | 77.4930 | 56.8749 | 97.0459 | 0.9736 | 0.9540 |
| (ACO) | Sw07, Sw09, Sw14, Sw32, Sw37 | 76.6112 | 56.2071 | 95.9484 | 0.9742 | 0.9540 |

TABLE 6
The 33-bus network results with load factor $\gamma = 0.875$

| Approaches | Open state | $TPL$ $(kW)$ | $TQL$ $(kVar)$ | $TSL$ $(kVA)$ | $V_{av}$ $(p.u.)$ | $V_{min}$ $(p.u.)$ |
|---|---|---|---|---|---|---|
| Initial configuration | Sw33, Sw34, Sw35, Sw36, Sw37 | 152.2034 | 101.45 | 182.92 | 0.9553 | 0.9200 |
| (PSO) | Sw07, Sw09, Sw14, Sw28, Sw32 | 105.8680 | 79.3873 | 133.3817 | 0.9716 | 0.9490 |
| (ACO) | Sw07, Sw09, Sw14, Sw32, Sw37 | 105.5440 | 77.4382 | 132.1862 | 0.9698 | 0.9460 |

TABLE 7
The 33-bus network results with load factor $\gamma = 1.125$

| Approaches | Open state | $TPL$ $(kW)$ | $TQL$ $(kVar)$ | $TSL$ $(kVA)$ | $V_{av}$ $(p.u.)$ | $V_{min}$ $(p.u.)$ |
|---|---|---|---|---|---|---|
| Initial configuration | Sw33, Sw34, Sw35, Sw36, Sw37 | 261.6769 | 174.54 | 314.56 | 0.9414 | 0.9000 |
| (PSO) | Sw07, Sw09, Sw14, Sw28, Sw32 | 179.3664 | 134.5258 | 225.9923 | 0.9631 | 0.9335 |
| (ACO) | Sw07, Sw09, Sw14, Sw32, Sw37 | 178.8475 | 131.2352 | 224.0008 | 0.9606 | 0.9295 |

Table 8
The 33-bus network results with load factor $\gamma = 1.250$

| Approaches | Open state | $TPL$ $(kW)$ | $TQL$ $(kVar)$ | $TSL$ $(kVA)$ | $V_{av}$ $(p.u.)$ | $V_{min}$ $(p.u.)$ |
|---|---|---|---|---|---|---|
| Initial configuration | Sw33, Sw34, Sw35, Sw36, Sw37 | 329.8092 | 220.08 | 396.53 | 0.9342 | 0.8897 |
| (PSO) | Sw07, Sw09, Sw14, Sw28, Sw32 | 224.2545 | 168.2072 | 282.5558 | 0.9587 | 0.9256 |
| (ACO) | Sw07, Sw09, Sw14, Sw32, Sw37 | 223.6454 | 164.1153 | 280.1131 | 0.9560 | 0.9211 |

From Tables 5–8, it is noticed that the average voltage improved by decreasing $\gamma$ and the total active power loss was the minimum when $\gamma$ = 0.75, and was the maximum when $\gamma$ = 1.250. The voltage and the active power losses reduction profiles of the network (for the initial and optimal configuration), when ACO algorithm is applied for a different value of $\gamma$ are shown below.

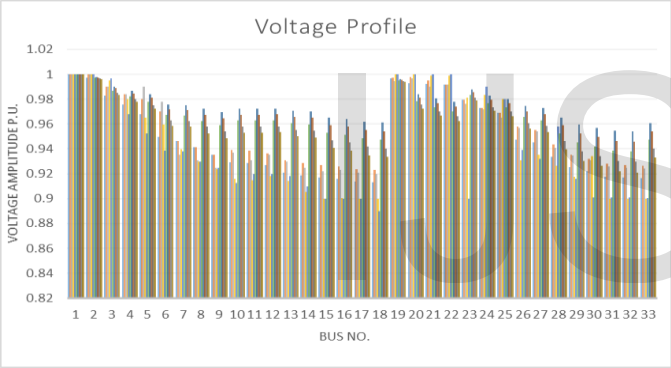


**Fig. 9:** Voltage profile for the 33-bus network (before and after re-configuration) using the ACO algorithm with different value of $\gamma$

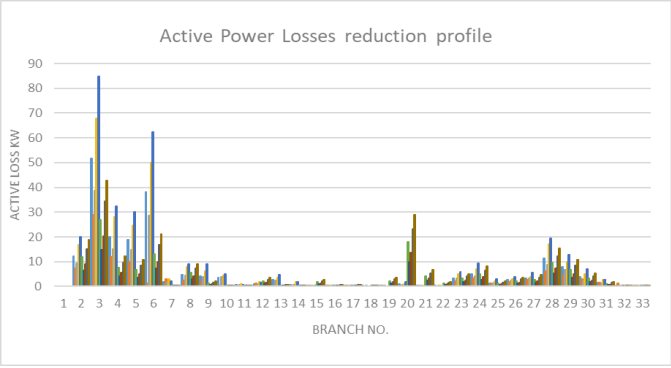


**Fig. 10:** Active power loss reduction profile for the 33-bus network (before and after re-configuration) using the ACO algorithm with different value of $\gamma$.

## 5.2 Optimal Re-configuration Results for Case 3

Tables 9-16 show a comparison between the re-configuration when ACO and PSO approaches applied for different load patterns (all seasons). It was noticed from these tables that the re-configuration pattern with switch set (Sw7, Sw9, Sw14, Sw32, Sw37) had the minimum TPL.

TABLE 9
The 33-bus network results with $\sigma = 0.72$ , $\tau = 2.96$

| Approaches | Open state | $TPL$ $(kW)$ | $TQL$ $(kVar)$ | $TSL$ $(kVA)$ | $V_{av}$ $(p.u.)$ | $V_{min}$ $(p.u.)$ |
|---|---|---|---|---|---|---|
| Initial configuration | Sw33, Sw34, Sw35, Sw36, Sw37 | 166.4666 | 110.6838 | 202.7482 | 0.9534 | 0.9216 |
| (PSO) | Sw07, Sw09, Sw14, Sw36, Sw37 | 123.4768 | 89.4825 | 153.9736 | 0.9675 | 0.9393 |
| (ACO) | Sw07, Sw09, Sw14, Sw32, Sw37 | 122.0906 | 89.7174 | 153.0014 | 0.9674 | 0.9429 |

TABLE 10
The 33-bus network results with $\sigma = 0.92$ , $\tau = 4.04$

| Approaches | Open state | $TPL$ $(kW)$ | $TQL$ $(kVar)$ | $TSL$ $(kVA)$ | $V_{av}$ $(p.u.)$ | $V_{min}$ $(p.u.)$ |
|---|---|---|---|---|---|---|
| Initial configuration | Sw33, Sw34, Sw35, Sw36, Sw37 | 156.9202 | 104.2283 | 191.0713 | 0.9548 | 0.9241 |
| (PSO) | Sw07, Sw11, Sw14, Sw32, Sw37 | 118.4284 | 87.0938 | 148.4241 | 0.9674 | 0.9444 |
| (ACO) | Sw07, Sw09, Sw14, Sw32, Sw37 | 117.0997 | 86.1006 | 146.7801 | 0.9681 | 0.9444 |

TABLE 11
The 33-bus network results with $\sigma = 1.04$ , $\tau = 4.19$

| Approaches | Open state | $TPL$ $(kW)$ | $TQL$ $(kVar)$ | $TSL$ $(kVA)$ | $V_{av}$ $(p.u.)$ | $V_{min}$ $(p.u.)$ |
|---|---|---|---|---|---|---|
| Initial configuration | Sw33, Sw34, Sw35, Sw36, Sw37 | 154.2558 | 102.4242 | 187.8050 | 0.9552 | 0.9248 |
| (PSO) | Sw07, Sw09, Sw14, Sw36, Sw37 | 116.8353 | 84.7342 | 145.7343 | 0.9684 | 0.9415 |
| (ACO) | Sw07, Sw09, Sw14, Sw32, Sw37 | 115.8059 | 85.1403 | 145.1532 | 0.9682 | 0.9448 |

TABLE 12
The 33-bus network results with $\sigma = 1.30$ , $\tau = 4.38$

| Approaches | Open state | $TPL$ $(kW)$ | $TQL$ $(kVar)$ | $TSL$ $(kVA)$ | $V_{av}$ $(p.u.)$ | $V_{min}$ $(p.u.)$ |
|---|---|---|---|---|---|---|
| Initial configuration | Sw33, Sw34, Sw35, Sw36, Sw37 | 149.3500 | 99.1019 | 181.7878 | 0.9560 | 0.9262 |
| (PSO) | Sw07, Sw09, Sw14, Sw36, Sw37 | 114.4098 | 82.9640 | 142.7024 | 0.9687 | 0.9423 |
| (ACO) | Sw07, Sw09, Sw14, Sw32, Sw37 | 113.4663 | 83.3909 | 142.2031 | 0.9686 | 0.9455 |

TABLE 13
The 33-bus network results with $\sigma = 1.25$ , $\tau = 3.50$

| Approaches | Open state | $TPL$ $(kW)$ | $TQL$ $(kVar)$ | $TSL$ $(kVA)$ | $V_{av}$ $(p.u.)$ | $V_{min}$ $(p.u.)$ |
|---|---|---|---|---|---|---|
| Initial configuration | Sw33, Sw34, Sw35, Sw36, Sw37 | 154.9251 | 102.8648 | 188.5960 | 0.9551 | 0.9247 |
| (PSO) | Sw07, Sw09, Sw14, Sw36, Sw37 | 117.7408 | 85.3154 | 146.8160 | 0.9683 | 0.9411 |
| (ACO) | Sw07, Sw09, Sw14, Sw32, Sw37 | 116.5930 | 85.6296 | 146.0838 | 0.9681 | 0.9444 |

TABLE 14
The 33-bus network results with $\sigma = 0.99$ , $\tau = 3.95$

| Approaches | Open state | $TPL$ $(kW)$ | $TQL$ $(kVar)$ | $TSL$ $(kVA)$ | $V_{av}$ $(p.u.)$ | $V_{min}$ $(p.u.)$ |
|---|---|---|---|---|---|---|
| Initial configuration | Sw33, Sw34, Sw35, Sw36, Sw37 | 156.3237 | 103.8218 | 190.3345 | 0.9549 | 0.9243 |
| (PSO) | Sw07, Sw09, Sw14, Sw36, Sw37 | 117.9920 | 85.5595 | 147.1682 | 0.9682 | 0.9411 |
| (ACO) | Sw07, Sw09, Sw14, Sw32 Sw37 | 116.9012 | 85.9357 | 146.5195 | 0.9681 | 0.9445 |

TABLE 15
The 33-bus network results with $\sigma = 1.50$ , $\tau = 3.15$

| Approaches | Open state | $TPL$ $(kW)$ | $TQL$ $(kVar)$ | $TSL$ $(kVA)$ | $V_{av}$ $(p.u.)$ | $V_{min}$ $(p.u.)$ |
|---|---|---|---|---|---|---|
| Initial configuration | Sw33, Sw34, Sw35, Sw36, Sw37 | 153.3544 | 101.7947 | 186.6510 | 0.9553 | 0.9252 |
| (PSO) | Sw07, Sw09, Sw14, Sw36, Sw37 | 117.3027 | 84.9442 | 146.2360 | 0.9683 | 0.9412 |
| (ACO) | Sw07, Sw09, Sw14, Sw32, Sw37 | 116.1109 | 85.2055 | 145.4362 | 0.9682 | 0.9445 |

TABLE 16
The 33-bus network results with $\sigma = 1.51$ , $\tau = 3.40$

| Approaches | Open state | $TPL$ $(kW)$ | $TQL$ $(kVar)$ | $TSL$ $(kVA)$ | $V_{av}$ $(p.u.)$ | $V_{min}$ $(p.u.)$ |
|---|---|---|---|---|---|---|
| Initial configuration | Sw33, Sw34, Sw35, Sw36, Sw37 | 151.7041 | 100.6802 | 184.6359 | 0.9556 | 0.9257 |
| (PSO) | Sw07, Sw09, Sw14, Sw36, Sw37 | 116.3255 | 84.2556 | 145.0300 | 0.9685 | 0.9415 |
| (ACO) | Sw07, Sw09, Sw14, Sw32, Sw37 | 115.1982 | 84.5536 | 144.3044 | 0.9683 | 0.9448 |

The voltage and the active power losses reduction profiles of the network (for the initial and optimal configuration), when ACO algorithm is applied for a different value of $\sigma, \tau$ are shown below.

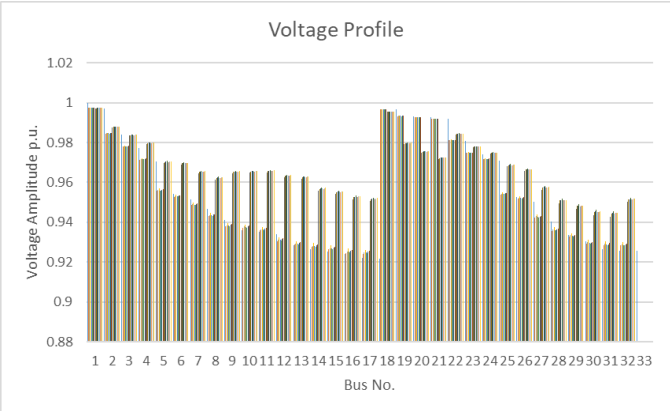


**Fig. 11:** Voltage profile for the 33-bus network (before and after re-configuration) using the ACO algorithm for different patterns with a different value of $\sigma, \tau$

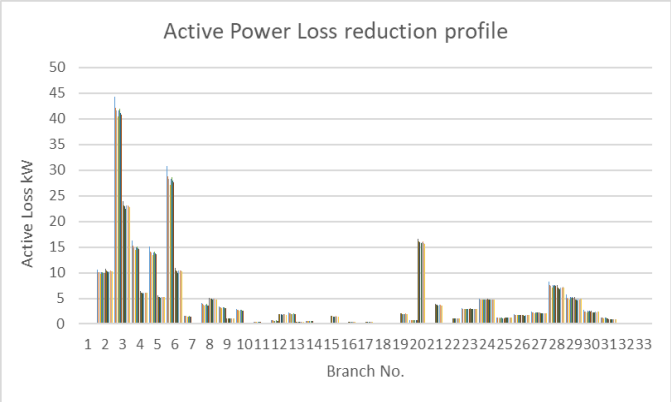


**Fig. 12:** Active power loss reduction profile for the 33-bus network (before and after re-configuration) using the ACO algorithm for different patterns with a different value of $\sigma, \tau$

## 6 CONCLUSIONS

The main focus of this research is to examine the load model optimization problem from different perspectives (residential and industrial) load types to reflect variable load styles with variable exponential rates. In addition, to test the effectiveness of the proposed ant colony optimization and particle swarm optimization algorithms when re-configuring electrical distribution networks in order to minimize system power loss and voltage profile improvement. In this work, we described the construction of the Ant Colony Optimization (ACO) and the Particle Swarm Optimization (PSO) techniques. As the algorithms involves a probability-based search, the decision of ACO and PSO algorithms is simple and show better performance with significant reduction in the computation effort, as they search for the optimal solution. The parameters of the proposed methods (ACO) and (PSO) are adjusted by trial and error in order to achieve the maximum efficiency of the proposed algorithm in order to obtain an optimal solution. The ACO and PSO methods have been applied to a standard 33-bus test system to minimize total line losses without violating operating constraints. The framework has been designed, programmed and implemented using the MATLAB R2017b environment. Total actual, reactive and apparent power losses, average voltage and minimum voltage were determined at each stage. Based on the results obtained for the test system show clearly the power loss reduction after re-configuration.

## 7 REFERENCES

[1] T. Q. D. Khoa, Member, IEEE, and B. T. T. Phan, "Ant Colony Search - based Loss Minimum for Reconfiguration of Distribution Systems", Electrical and Electronics Engineering, Hochiminh University of Technology, Vietnam ,2006.

[2] S. Kalamben and G. Agnihotri, "Loss minimization techniques used in distribution network: bibliographical survey", Reviews Volume, January 2014, Pages 184-200.

[3] A. M. Imran and M. Kowsalya, "A new power system reconfiguration scheme for power loss minimization and voltage profile enhancement using Fireworks Algorithm", International Journal of Electrical Power & Energy Systems, Volume 62, November 2014, Pages 312-322.

[4] M. Assadian, M. M. Farsangi and H. Nezamabadi-pour, "distribution network reconfiguration for loss reduction using particle swarm optimization", TPE-06 3rd International Conference on Technical and Physical Problems in Power Engineering May 29-31, 2006, Ankara, turkey.

[5] S. Essallah and A. Khedher, "Optimal Distribution System Reconfiguration for Loss Minimization using BPSO Algorithm", The 10th International Renewable Energy Congress (IREC 2019).

[6] A Merlin and B Back, "Search for a minimal-loss operating spanning tree configuration in an urban power distribution system", In: Proceedings of power system computation conference (PSCC); Cambridge 1975, Paper 12/6.

[7] J. Olamaei, G. Gharehpetian, and T. Niknam, "An approach based on particle swarm optimization for distribution feeder reconfiguration considering distributed generators", in Power Systems Conference: Advanced Metering, Protection, Control, Communication, and Distributed Resources, IEEE, pp. 326–330, 2007.

[8] D. Zhang, Z. Fu, and L. Zhang, "An improved ts algorithm for loss minimum reconfiguration in large-scale distribution systems", Electric Power Systems Research, vol. 77, no. 5-6, pp. 685–694, 2007.

[9] T. Taylor and D. Lubkeman, "Implementation of heuristic search strategies for distribution feeder reconfiguration", IEEE Transactions on Power Delivery, vol. 5, no. 1, pp. 239–246, 1990.

[10] V. Parada, J. A. Ferland, M. Arias, and K. Daniels, "Optimization of electrical distribution feeders using simulated annealing, ", IEEE Transactions on Power Delivery, vol. 19, no. 3, pp. 1135–1141, 2004.

[11] J. Y. Fan, L. Zhang, and J. D. McDonald, "Distribution network reconfiguration: single loop optimization", IEEE transactions on Power Systems, vol. 11, no. 3, pp. 1643–1647, 1996.

[12] A. Abdelaziz, R. Osama, and S. El-Khodary, "Reconfiguration of distribution systems for loss reduction using the hyper-cube ant colony optimization algorithm", IET generation, transmission & distribution, vol. 6, no. 2, pp. 176–187, 2012.

[13] F. M. F. Flaih, X. Lin, M. K. Abd, S. M. Dawoud, Z. Li and O. S. Adio, "A New Method for Distribution Network Reconfiguration Analysis under Different Load Demands", Energies 2017, 10, 455.

[14] V. Borozan, D. Rajicic and R. Ackovski, "Minimum loss reconfiguration of unbalanced distribution networks", IEEE Transactions on Power Delivery, Vol. 12, No. 3, 1997, pp. 435-447.

[15] A. Savio, F. Bignucolo, R. Sgarbossa, P. Mattavelli, A. Cerretti and R. Turri, "A novel measurement-based procedure for load dynamic equivalent identification". In Proceedings of the 2015 IEEE 1st International Forum on Research and Technologies for Society and Industry Leveraging a better tomorrow (RTSI), Torino, Italy, 16–18 September 2015.

[16] W. W. Price, H. D. Chiang, H. K. Clark and E. Vaahedi, "Load representation for dynamic performance analysis of power systems", IEEE Trans. Power Syst. 1993, 8, 472–482.

[17] I. V. Milanovic´, J. Matevosiyan, A. Borghetti, S. Z. Djokic and Z. Y. Dong, "Modelling and Aggregation of Loads in Flexible Power Networks", CIGRE Technical Brochure 566; CIGRE: Paris, Frace, 2014.

[18] S. M. Mousavi, and H. A. Abyaneh, "Effect of load models on probabilistic characterization of Aggregated load patterns", IEEE Trans. Power Syst. 2011, 26, 811–819.

[19] M. Dorigo, "Optimization, learning and natural algorithms", Ph.D. dissertation, Dep. Elec. Eng., Univ. of Milano, Italy, 1992.

[20] M. Dorigo and L. M. Gambardella, "Ant algorithm for discrete optimization ", Institute of technology", Artificial Life, Vol. 5, No. 2, 1999, pp. 137-172.

[21] M. R. Nayak, "Optimal Feeder Reconfiguration of Distribution System with Distributed Generation Units using HC-ACO",

International Journal on Electrical Engineering and Informatics - Volume 6, Number 1, March 2014.
[22] C.-F. Chang "Reconfiguration and Capacitor Placement for Loss Reduction of Distribution Systems by Ant Colony Search Algorithm", IEEE transactions on power systems, vol. 23, no. 4, November 2008.
[23] J. Kennedy and R. Eberhart, "Particle swarm optimization", in Proc. 1995 IEEE Neural Networks Conf., IEEE Service center, Piscataway, NJ, pp. 1942-1948.
[24] M. H. Moradi and M. Abedini, "A combination of genetic algorithm and particle swarm optimization for optimal DG location and sizing in distribution systems", International Journal of Electrical Power & Energy Systems, vol. 34, no. 1, Jan. 2012, pp. 66-74.
[25] Lalitha M. Padma, Reddy V. C. Veera,Usha V., Reddy N. Sivarami, "Optimal DG Placement for Minimum Real Power Loss in Radial Distribution System using PSO", ARPN Journal of Engineering and Applied Sciences 2010, Vol. 5, No. 4, pp. 30-37.
[26] J. Robinson, and Y. Rahmat-Samii, "Particle swarm optimization in electromagnetics" IEEE Trans. Antennas and Propagation, vol. 52, no. 2, pp.397-407, Feb. 2004.
**[27]** Y. Shi and R.C. Eberhart, "**Parameter selection in particle swarm optimization**", Evolutionary programming VII (1998), Lecture Notes in computer science 1447. pp.591~600. springer 1998.
**[28]** M. A. A. Pedrasa, Student Member, IEEE, Ted D. Spooner, and I.F. MacGill, "**Scheduling of Demand Side Resources Using Binary Particle Swarm Optimization**" IEEE transactions on power systems, vol. 24, no. 3, august 2009.
**[29]** T.T. Nguyen, A. V. Truong, "Distribution network reconfiguration for power loss minimization and voltage profile improvement using cuckoo search algorithm". Int. J. Electr. Power Energy Syst. 2015, 68, 233–242v.
**[30]** S. Essallah, A. Bouallegue and A. Khedher, "**Optimal sizing and placement of DG units in radial distribution system**", International Journal of Renewable Energy Research, vol. 8, no. 1, pp. 166-177, 2018.